The Holocene 16,5 (2006) pp. 635–646

A late-Holocene record of loess deposition in ice-wedge polygons reflecting wind activity and ground moisture conditions, Bylot Island, eastern Canadian Arctic

Daniel Fortier,[1]* Michel Allard[2] and Frédérique Pivot[3]

([1]Institute of Northern Engineering and Department of Civil and Environmental Engineering, College of Engineering & Mines, P.O. Box 755900, University of Alaska Fairbanks, Fairbanks AK 99775-5900, USA; [2]Geography Department and Centre d'études nordiques, Université Laval, Québec, Canada; [3]Geography Department, York University, Ontario, Canada)

Received 4 April 2005; revised manuscript accepted 11 November 2005

A HOLOCENE RESEARCH PAPER

Abstract: On Bylot Island, a field of tundra polygons at the margin of a glacial outwash plain contains a well-preserved syngenetic permafrost sequence of ground ice and alternating loess and organic layers that was accumulated during the late Holocene. Periods of increased deposition of loess alternated with periods of growth of bryophytes during the last 3500 years. These shifts in soil accretion regime are interpreted in terms of significant shifts of the summer surface wind conditions and active layer moisture regime (Precipitation–Evaporation or P–E), in response to regional climatic variations and recurrent changes of atmospheric circulation. There was a high level of variability and large amplitude of the P–E regime and summer surface wind conditions on a decennial and secular timescale in general. However, according to the Greenland GISP2 bi-decennial oxygen isotopes data, there was a low variability and amplitude (by a few degrees centigrade or less) of the regional mean annual air temperature. From 2950 to 2750 cal. BP, the summer climate was warmer and had the strongest and most frequent northwesterly surface winds of the late Holocene. Shifts to a weaker northwesterly summer surface wind activity preceded the dryer episodes that occurred from 2750 to 2450 and around 1850 cal. BP. Major wetter episodes occurred from 2450 to 2350, around 2050, from 1750 to 1550, from 1350 to 1150 and from 550 to 250 cal. BP. There is no clear relationship between P–E or summer surface wind regimes and air temperatures. Shifts of late Holocene summer aeolian regime can probably be better explained by the recurrence of particular synoptic circulation types in response to changes in the position of the atmospheric eastern Canadian Polar Trough.

Key words: Atmospheric circulation, active-layer moisture, Canadian Polar Trough, ice-wedge polygons, late Holocene, loess, palaeoclimate, permafrost, Bylot Island.

Introduction

Syngenetic ice-wedge polygons occur in many regions across the Arctic. The soil in their centres often consists of frozen sequences of organic accumulation and mineral sediments originating from aeolian, fluvial (floods) or slope processes. Therefore, they provide a potential stratigraphic record of past environmental conditions. Some palaeoclimatic reconstructions have been attempted already by several authors from such sedimentary environments (eg, Lafarge-England *et al.*, 1991; Seppälä *et al.*, 1991; Garneau, 1992; Kasper and Allard, 2001). On the southwestern part of Bylot Island (Figure 1A, B), a field of tundra polygons at the margin of a sandur is a site that offers the possibility to reconstruct wind and active layer moisture palaeoconditions because the permafrost contains a well-preserved sequence of alternating loess and organic layers. Records of late Holocene climate conditions are sparse from this part of the eastern Canadian Arctic. The aim of this paper is to document changes in wind regime and active-layer moisture on Bylot Island during the Neoglacial.

*Author for correspondence (e-mail: ffdf@uaf.edu)

10.1191/0959683606hl960rp

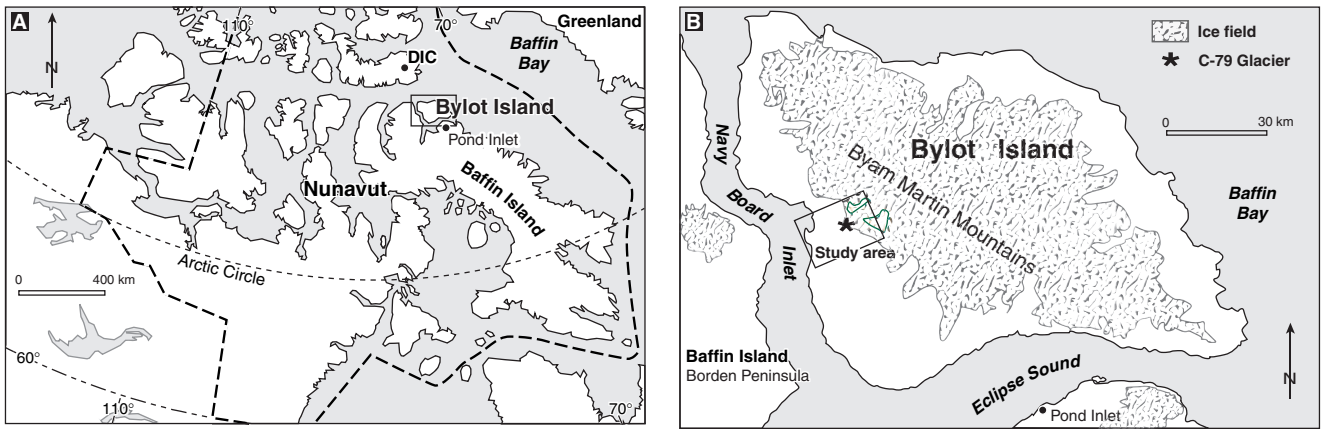

Figure 1 Location of the study site. (A) Bylot Island, eastern Canadian Arctic archipelago (dotted line: Nunavut). DIC, Devon Island Ice Cap. (B) The study site is located on the southern plain of Bylot Island in the valley of glacier C-79

Regional climate

The High Arctic climate is regarded as more sensitive to the variations of atmospheric circulation than that of other Northern Hemisphere areas because of large potential changes in feedback effects (Pryzbylak, 2000). A reorganization of the atmospheric circulation, even on a small scale, often involves a change in the trajectories of air masses and, consequently, a change of wind and precipitation regimes and therefore of soil-moisture conditions (Taylor *et al*., 1993; Kapsner *et al*., 1995). The climate of the eastern Canadian Arctic archipelago is characterized by large regional variations in temperature and precipitation (Alt and Maxwell, 2000). The position of the Canadian Polar Trough (CPT), a low-pressure feature of the Baffin and Bylot Islands region, is a primary determinant of the atmospheric circulation over the study site (Shabbar *et al*., 1997). Longitudinal displacement of the CPT under the North Atlantic Oscillation (NAO) forcing, which can be viewed as the regional expression of the Artic Oscillation (AO) (Hurrell, 1995; Shabbar *et al*., 1997; Pryzbylak, 2000; Serreze *et al*., 2000; Marshall *et al*., 2001), leads to atmospheric circulation changes. These changes are associated to different cyclonic patterns and storm tracks (Maxwell, 1980; Alt and Maxwell, 1990; Kapsner *et al*., 1995; Marshall *et al*., 2001). The resultant synoptic types are thus responsible for the air temperature and precipitation regimes at the study site (Frei and Robinson, 1999; Alt and Maxwell, 2000; Serreze *et al*., 2000; Barlow, 2001; Bonsal *et al*., 2001; New *et al*., 2001; Bamzai, 2003). On Bylot Island, most of the precipitations fall as snow. The AO and NAO are mainly cold-season patterns, although they are also observed in summer air temperature, surface wind regime and cyclonic activity (Mote, 1998a,b; Pryzbylak, 2000). In summer, the decrease in the latitudinal temperature gradient gives rise to a strengthening of zonal atmospheric circulation. On Bylot Island and Northeast Baffin Island, the climatic conditions are then influenced by the atmospheric circulation (50 kPa) coming from the northwest (Maxwell, 1980; Alt and Maxwell, 1990, 2000) that generate dominant winds from that direction.

The present-day climate is best described from the late twentieth century meteorological record from Pond Inlet (72°40′N, 77°58′W), a settlement located about 85 km southeast of the study site (Figure 1B). The village has a polar climate with a slight maritime influence (Maxwell, 1981). The mean annual air temperature (1971–2000) was −15.1°C (Environment Canada, 2002). There is an excellent correlation between the air temperatures of Pond Inlet and Bylot Island (Fortier and Allard, 2005). Monthly mean air temperatures are 1.8°, 6° and 4.2° C for June, July and August, respectively (Environment Canada, 2002). The annual precipitation is 191 mm/yr of which 145 mm water equivalent falls as snow (Environment Canada, 2002). The snowmelt period generally lasts from the end of May through June, although some residual patches can last throughout the summer. Bylot Island is well into the continuous permafrost zone, the permafrost being probably over 400 m thick (Maxwell, 1980).

Previous stratigraphic study of Holocene soils (Allard, 1996) and palaeovegetation record clearly show that this high Arctic site always experienced very cold tundra conditions. Past climate changes are more likely to be reconstructed through shifts in physical (ie, geomorphological) processes rather than through standard palaeoecological plant macrofossils analyses (eg, Ellis and Rochefort, 2004).

Study site

The study site is located on the southern plain of Bylot Island, in the valley of glacier C-79 (Inland Waters Branch, 1969) (see Allard, 1996, for a general map of the valley), locally called Qarlikturvik (Figure 1B). A river runs through braided channels in the sandur that fills the bottom of the valley. The river runs NE–SW and is bordered on its southern side by an aggradation terrace that has an elevation of about 15 m a.s.l. at the study site. The terrace is approximately 3–4 m above the outwash surface and is not inundated during high water stages of the proglacial river. The river regime shows marked diurnal fluctuations and day to day variability in response to the melting rate of glacier C-79, which allow for deposition of the sediments. Exposed fine-grained sediments on alluvial bars are readily eroded and often seen remobilized under wind deflation. Fortier and Allard (2004) demonstrated that the terrace has been aggrading since around 4000 cal. BP (calibrated radiocarbon years) (Table 1: UL-2356) after the retreat of the valley glacier to its current upstream location. The terrace is crossed by networks of ice-wedge polygons. Many of the polygons form closed central depressions. The latter are generally very wet and many of them contain ponds. Plant communities are primarily made up of mosses and hydrophilic graminoids that occupy the centre of the polygons (Massé, 1998). They are relatively homogenous and dominated by grasses such as *Dupontia fisheri* and *Pleuropogon sabinei* and sedges such as *Carex aquatilis* var. stans, *Eriophorum scheuchzeri* and *Eriophorum angustifolium.* On the ridges, the surface is

Table 1 Radiocarbon dates.

Laboratory no.[a]	Material[b]	Years BP[c]	Cal. years BP	Interval[d]	Depth[e] (m)
Polygon A[f]					
UL-2355	Peat macrofossils	Modern	>0	AD 1950–1999	Surface
UL-2270	Peat macrofossils	580 ± 90	618	689–466	0.3
UL-2200	Peat macrofossils	790 ± 90	691	917–634	0.32
UL-2327	Peat macrofossils	980 ± 90	925	1060–701	0.35
UL-2203	Peat macrofossils	1350 ± 90	1287	1417–1056	0.87
UL-2258	Peat macrofossils	1670 ± 90	1553	1743–1186	0.93
UL-2315	Peat macrofossils	2040 ± 90	1993	2184–1817	1.11
UL-2314	Peat macrofossils	2410 ± 90	2359	2745–2309	1.38
UL-2335	Peat macrofossils	2610 ± 70	2749	2868–2467	1.79
UL-2328	Peat macrofossils	2750 ± 90	2849	3081–2735	2
UL-2356	Salix twigs and peat macrofossils	3670 ± 110	3983	4299–3693	2.33
Polygon B[f]					
UL-2195	Peat macrofossils	240 ± 80	294	470–240	0.07
UL-2202	Peat macrofossils	290 ± 70	310	506–268	0.1
UL-2197	Peat macrofossils	300 ± 90	313	519–255	0.12
UL-2316	Peat macrofossils	1260 ± 90	1179	1308–1045	0.27
UL-2265	Peat macrofossils	1410 ± 90	1304	1523–1169	0.35
UL-2189	Peat macrofossils	1860 ± 90	1819	1953–1586	0.57
UL-2151	Peat macrofossils	1960 ± 90	1912	2127–1705	0.74
UL-2168	Peat macrofossils	2020 ± 90	1980	2161–1771	0.88
UL-2194	Peat macrofossils	2370 ± 90	2353	2725–2301	1.2
UL-2169	Peat macrofossils	2430 ± 90	2415	2743–2335	1.31
UL-2170	Peat macrofossils	2450 ± 90	2470	2754–2330	1.43
UL-2150	Peat macrofossils	2760 ± 80	2852	3071–2748	1.95
UL-2149	Peat macrofossils	2780 ± 80	2867	3077–2751	2.08
UL-2152	Salix twigs and peat macrofossils	3270 ± 100	3472	3722–3319	2.41
Allard (1996)					
UL-1338	Peat macrofossils	Modern	>0	AD 1950–1993	Surface
UL-1033	Peat macrofossils	1050 ± 90	953	1014–892	1.1
UL- 1048	Peat macrofossils	2210 ± 120	2299	2340–2107	1.35
UL-1034	Peat macrofossils	2510 ± 90	2564	2610–2468	2.3
UL-1035	Peat macrofossils	2600 ± 90	2471	2781–2703	2.5
UL-1025	Peat macrofossils	2900 ± 90	3014	3082–2920	3.2
Klassen (1982)					
GSC-3227	Salix twigs	120 ± 80	97	163–0	–

[a]UL, Laval University (Canada); GSC, Geological survey of Canada.
[b]Type of organic matter dated.
[c]Uncalibrated years before the present (1950).
[d]Confidence interval 95–99%.
[e]Depth: depth of the sample from the surface of the polygon.
[f]Dates used for the chronostratigraphic models.

better drained and there is a greater cover of mesic species including shrubs such as *Salix arctica*, forbs (less than 2%) such as *Cassiope tetragona* and grasses such as *Alopecurus alpinus*, *Arctagrostis latifolia* and *Poa arctica* (Duclos, 2002).

The studied polygons are located in the centre of the terrace about 100 m from a thermokarst lake that intercepts run-off from the valley slopes. The polygons are low-centred and roughly look like 18 m (polygon A) and 14 m (polygon B) long rectangles, respectively (Figure 2B). The polygons' ridges are large, with a width up to 10 m and a height up to 80 cm. The polygons are hydrologically independent, so that the active-layer moisture results essentially from precipitation inputs (snow and rain), evaporation and summer thaw of the active layer rather than surface run-off or groundwater flux. The interannual variability of the active-layer moisture content can be high. Indeed, sunny, warm, dry or windy summers can cause high evaporation and the partial drying of these polygon centres. The water content of the active layer therefore represents the polygon's water balance, that is to say the balance between precipitation inputs (snow and rain) and evapotranspiration outputs (surface water evaporation and plant transpiration). When the proglacial river is at low stage the winds from the northwest blow across the surface of the sandur and transport loess, which are afterwards deposited on the southern terrace. Field observations of freshly deposited loess on the surface of the polygons indicate that loess deposition and organic accumulation in the centre of the polygons occur syngenetically (Figure 2A). This sedimentation causes the surface of the polygons and the permafrost table to rise in phase over the years. Surface accretion prevents thawing of the basal part of the active layer and results in the progressive integration of sediments and ground ice in the permafrost (Mackay, 1975, 1990).

Our hypothesis is that the sedimentation of loess, the accumulation of peaty organic matter and accretion of ground ice as observed today on the terrace are recorded in the permafrost of the polygons being studied. Changes that eventually took place in the factors that controlled these processes, particularly wind directions and active layer moisture, should be recorded in the polygon stratigraphy. The

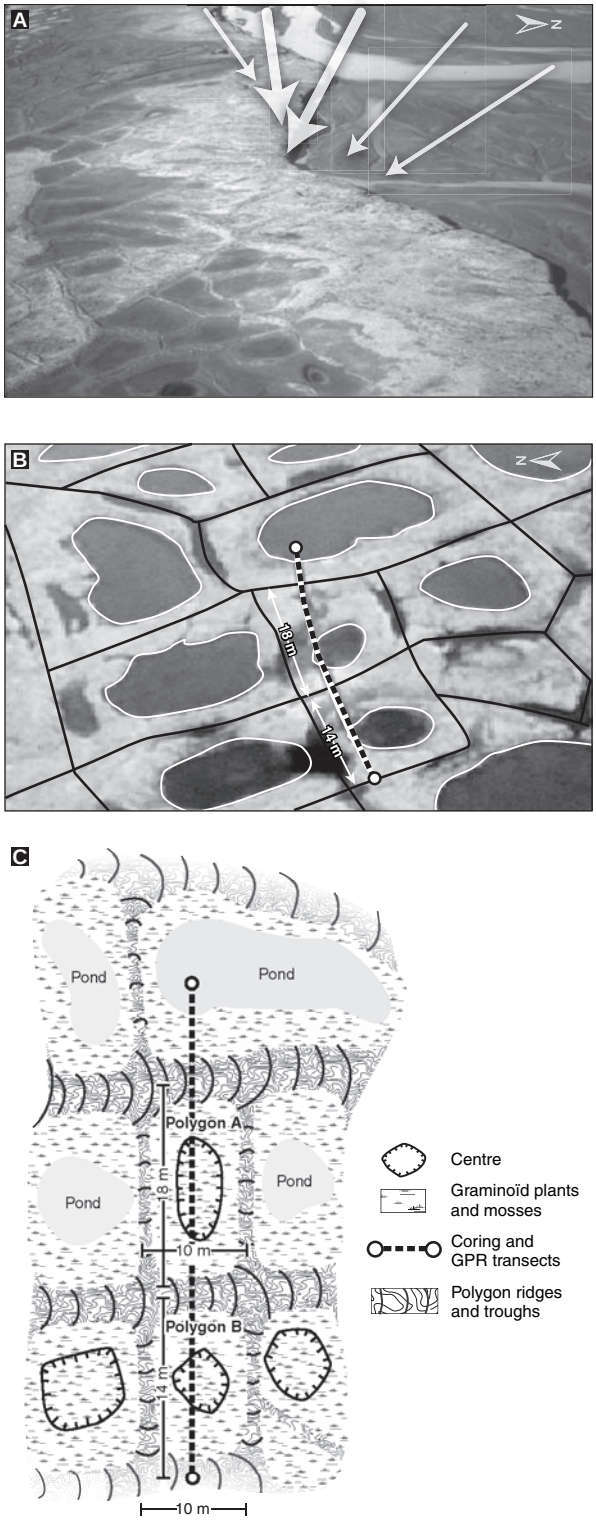

Figure 2 (A) Freshly deposited loess on the surface of the polygons (July 1999). The loess is blown from the sandur (upper right corner) during low-water stages of the proglacial river. The arrows show the average summer wind direction as measured on the terrace by a meteorological station. Thicker arrows show most frequent wind directions (see Figure 5C and D). (B) Oblique air photograph of the polygon field. (C) Schematic representation of polygons A and B showing the coring and GPR transects.

particular environmental configuration of the study site makes it possible to reconstruct the palaeowind regime and palaeoactive layer moisture conditions that prevailed during the late Holocene through comprehensive sedimentological and geocryological analyses of the polygons' sedimentary sequences.

Methodology

Ascertaining the original stratigraphy

In most ice-wedge polygons, the sedimentary strata and soil layers are deformed and thrusted upward along ice wedges (Mackay 1980, 2000). Also, new ice wedges may form within polygons if climatic and mechanical conditions leading to cracking and subdivision of existing polygons arise. It was therefore necessary to ensure that the sedimentary strata of peat, loess and ice in the studied polygons were not deformed by such periglacial processes. A series of holes were drilled at 2 m spacing interval along a transect across two polygons. In a previous paper, Fortier and Allard (2004) demonstrated that the layering was observed to be continuous in the centres of the polygons. It appeared that each polygon was indeed a bowl-shaped sedimentary basin, at the centre of which the layers are not affected by any deformations that would have led to stratigraphic inversions and dating errors resulting from dipping or reversed strata (Figure 2B, C). This was later confirmed by running a ground penetrating radar (GPR) survey along the transect (see pp. 16 and 164 in Fortier (2005) for GPR details).

Loess and water contents determination

Loess and water contents of the palaeoactive layer were measured in the cores retrieved from boreholes drilled in the centre of the two polygons (Figure 2C, 3). The core samples of these polygons were transported to the base camp where they were kept frozen. In the laboratory, a cryostratigraphic description of the cores was made. The cores were cut in 2 cm thick sections for laboratory analyses. The total gravimetric water (ice) content was obtained through oven drying (90°C, 72 h). The gravimetric loess content was obtained by eliminating the organic matter through loss on ignition (800°C, 20 min). The ice and loess contents between two samples analysed in the laboratory were interpolated with a spline function, assuming a constant accumulation rate between them. Some samples from the base of polygon B were broken during drilling, which limited the depth of this record.

Chronostratigraphic model

A time–depth curve was achieved by dating the core samples. The organic matter was extracted from the sediments by sieving and peat macrofossils were radiocarbon-dated. The age obtained was assigned to a depth equivalent to half the depth interval of the sample used for the dating. Assuming a constant accumulation rate between the dated levels, the depth and radiocarbon ages between two successive dates were interpolated linearly. The dates were calibrated to a 99% or 95% confidence interval following the method proposed by Stuiver and Reimer (1993) and Stuiver *et al*. (1998). The chronostratigraphic model was applied to the loess content data to convert depth to time as aeolian sedimentation took place syngenetically with the accumulation of organic matter (see Figure 5A, B in Fortier and Allard, 2004).

Reconstructing loess sedimentation and water content

A simple procedure was applied to the water content data of the cores to convert depth to time. The ice content of the core samples taken below the actual permafrost table represents the quantity of water contained at the bottom of the active layer at a given period, before it ultimately froze. Indeed, in response to syngenetic surface sedimentation and permafrost table elevation, the active layer gradually becomes an integral part of the permafrost. For reconstruction

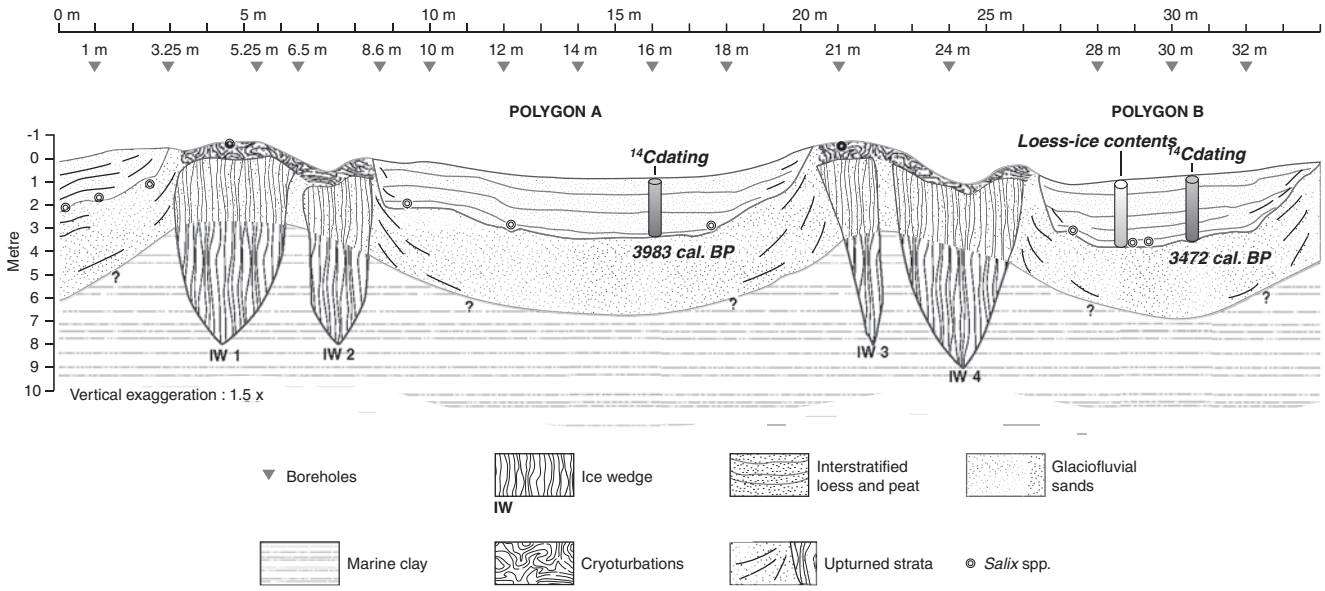

Figure 3 Stratigraphic reconstruction of polygons A and B using data from boreholes, cross-sections, GPR profiles, sedimentological analyses and radiocarbon data (adapted from Fortier and Allard, 2004 and Fortier, 2005)

purposes, we assume that the mean thickness of the active layer remained nearly constant over the accumulation period, although there has undoubtedly been some interannual variability (Romanovsky and Osterkamp, 1997; Zhang and Stamnes, 1998; Serreze *et al.*, 2000). Indeed, during the 1999 to 2003 period, the thickness of the active layer, as measured with a thermistor cable inserted in the centre of a low-centre polygon located on the terrace about 300 m away from the study site, varied from 37 to 49 cm. These variations in the depth of thaw can have resulted in a distortion of the precipitation–evaporation signal in the stratigraphy. During exceptionally warm summers, the active layer will be thicker thus melting ice at the permafrost table and releasing water. At the same time, warmer summers also increase evaporation in the active layer and the resulting water balance can be highly variable. However, if the accumulation rate was rapid and the climate fairly cold during the study period, the ice contents probably reflect better the high variability of the effective precipitation regime (Precipitation–Evaporation or P–E) rather than active-layer depth variability (Gajewski *et al.*, 1995, Frei and Robinson, 1999, New *et al.*, 2001; Serreze *et al.*, 2000).

The long-term thickness of the active layer was considered to be approximately 40 cm (Fortier and Allard, 2005). Depth was converted into time by assuming that the age of ground ice at the bottom of the palaeoactive layer roughly corresponds to the age of the polygon surface at that time, or the age of the peat located 40 cm higher up in the profile. The loess and water contents time series were used to establish anomaly curves, showing the deviation of the loess and water contents from the average of all the data from the site. Anomalies are departures of more than 1 or 2 standard deviations (σ) from the average.

Present-day wind regime and loess sedimentation period

From 1994 to 2003, the wind regime in the valley was measured at 3 m above the ground surface at a meteorological station located on the terrace, about 1.5 km from the study site. Wind speed and direction were measured at 60 s intervals using an anemometer (RM Young) and one random sample per hour was recorded by a CR10X datalogger (Campbell Scientific™). In order to obtain monthly averages for wind direction, each observation of wind direction was computed as a vector, where the vector length is the wind speed and the vector orientation is the wind direction. The mean vector was then computed for each season (Figure 5C) (Gagnon *et al.*, 2004).

In the springs of 1999, 2001 and 2002, just prior to snowmelt, snow pits were dug at several sites on the sandur and on the adjacent terraces to evaluate wind transport and loess sedimentation during the winter. A snow depth sensor, installed beside the meteorological station in 2001, provides a record of the build-up of the snow cover and its disappearance in spring.

Late Holocene GISP2 oxygen isotopes and regional air temperature reconstructions

Given the relative proximity of Bylot Island and the Greenland Ice Sheet Project 2 (GISP2) drilling site on Greenland (72°36′N, 38°30′W), the changes (0.5–0.6‰ per °C) in the oxygen isotope bidecennial signal ($\delta^{18}O_{20y}$) are probably a fair proxy for the air temperature trends (warming, cooling, stability) taking place at the study site (Grootes *et al.*, 1993; Kapsner *et al.*, 1995; Stuiver *et al.*, 1995, 1997; Greenland Summit Ice Cores CD-Rom (GSIC), 1997; Stuiver and Grootes, 2000; Lockwood, 2001). Nevertheless, the GISP2 site is about 3000 m a.s.l. whereas the study site is close to sea level and, therefore, a certain discrepancy and time lag might exist in the temperature records between the two sites. A $\delta^{18}O_{20y}$ anomaly curve, helpful to identify warmer and colder episodes, was realized by plotting the deviation of GISP2 values from the average for the period covered by the reconstruction in our study as a function of time.

Results

Stratigraphy and structure of the polygons

The ice wedges forming the polygons have widths of nearly 4 m at the permafrost table. The upper part of the ice wedges forms a roughly rounded bulge, indicating a syngenetic development (Figure 4). Two main stratigraphic units compose the upper 3 m of permafrost. From the surface down to approximately 2.5 m, a syngenetic ice-rich accumulation of fibrous peat mixed with medium poorly sorted wind-blown

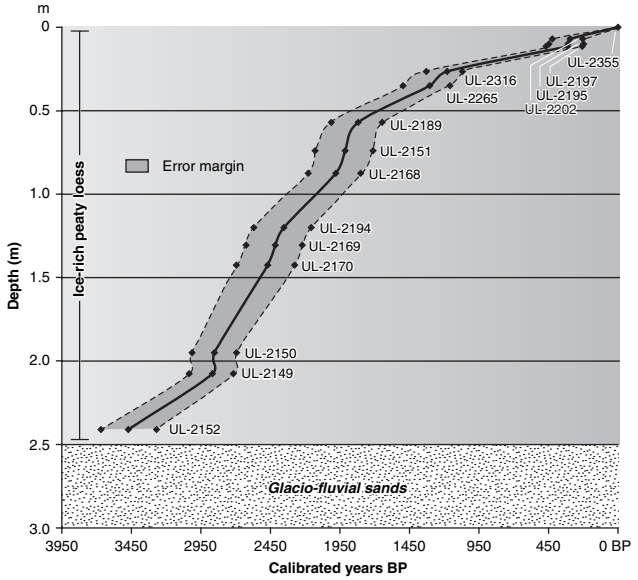

Figure 4 Chronostratigraphic model. The solid line is the syngenetic accumulation of the peaty loess within polygon B. Ages are in calibrated radiocarbon years BP. The grey zone between the dotted lines is the 99% confidence interval. The laboratory numbers of the radiocarbon dates are given for each point of the curve. See Table 1 for radiocarbon details

silt (loess) overlies glaciofluvial fine sands deposited before 3270 ± 100 BP (Table 1: UL-2152). Along the ice wedge sides, the sedimentary layers are curved upwards, reaching the surface in the ridges. Yet, in the central zone of the polygons, the sedimentary layers are subhorizontal, subparallel and not deformed (See Figure 5B in Fortier and Allard, 2004).

Chronostratigraphic model and accumulation rate

In the centre of polygons A and B, the basal dates of the peaty loess sequence are respectively 3670 ± 110 BP (235 cm) and 3270 ± 100 BP (241 cm) (Table 1: UL-2152, UL-2356). Within both polygons, sedimentary deposition is continuous and no date inversions were detected. Table 1 lists the samples used for radiocarbon dating, their characteristics and respective age. The age intervals of the radiocarbon dates overlap at several points along the stratigraphic profile, thus providing a good chrono-stratigraphic framework. The average rate of accumulation in the polygons was approximately 0.6 and 0.7 mm/yr for polygons A and B, respectively. A highly significant correlation ($R = 0.96$) exists between the chronostratigraphic models of both polygons for the last 3500 years, which indicates that sedimentation in both polygons occurred synchronously (see pp. 53 and 164 in Fortier, 2005). Indeed there were no significant gaps in the accumulation rate variations from one polygon to the next. With minute differences, the sediments and ice sequence is the same in both polygons, a fact that yields confidence in the validity of the palaeoenvironmental signal in the record. The chronostratigraphic model of polygon B (Figure 5) was constructed with 15 dates and is more precise and more representative of the sedimentation than that of polygon A, where only 11 dates were used.

Late Holocene loess sedimentation and P–E anomalies time series

The snowpits excavated on the sandur showed that only the basal layer of snow (10 cm) comprised wind-blown sands and silts. Indeed, above this layer and up to the surface, the snow is generally free of wind-blown sediments. On the terrace, the snowpack generally contains very little loess. Wind erosion on the sandur, transport and sedimentation of loess, therefore, essentially take place during June, July and August, before the establishment of a complete snow cover in the valley. Data from the snow depth sensor and from the Pond Inlet station (Environment Canada, 2002) show that snow already covers the ground of the valley by the end of August to early September. Grain size distribution of the loess is mainly a function of the sedimentary source (sandur) and it is relatively constant over the entire length of the cores (Figure 2B).

During the 1995–2000 period, the average annual wind speed was 1.95 ± 0.09 m/s (Cadieux *et al.*, 2005). Wind speeds were highest in summer (June, July, August), with an average daily wind speed of 2.92 ± 0.13 m/s, and particularly high in July with average daily wind speeds ranging from 1.8 to 4.2 m/s (Cadieux *et al.*, 2005). The dominant summer winds in the valley were blowing mainly from the West (262°) (Figure 5C, D). This is concordant with the dominant regional surface wind directions during summer (Alt and Maxwell, 1990) and in marked contrast with the other seasons. Observed data suggest that the westerly summer winds were therefore essentially responsible for the deposition of loess on the study site, which is located south (downwind) of the sandur that has an orientation SW–NE (Figure 2A, 5C, D).

The average of the $\delta^{18}O_{20y}$ values between 3450 cal. BP and the present (AD 1950) in the GISP2 record is $-34.84‰$ and the standard deviation (σ) is $0.34‰$. Figure 6C shows the variations in $\delta^{18}O_{20y}$ during the studied late Holocene period.

Because of sample loss at the base of the borehole in polygon B, the loess record covers the period from 3250 cal. BP up to the present. The average gravimetric loess content for this period is 72.4% and the standard deviation is 12.7%. Figure 6A shows the loess content anomaly curve in polygon B established for the late Holocene. Significant changes in loess content are interpreted when anomalies were equal to or greater (smaller) than one standard deviation above (below) the average. Reduction of the loess signal might result from higher sediment cohesion when the surface of the sandur is humid and from higher plant productivity (Vanderberghe, 1991; Garneau, 1992; Allard, 1996; McGowan *et al.*, 2003). Pore ice makes up the bulk of the ice of the core samples but some millimetre-thick ice lenses are also present. Because of sample loss at the base of the borehole, the water content reconstruction covers the period from 2775 cal. BP (depth of 190 cm) to AD 1950 (present) (depth of 41 cm). The average gravimetric water content for this period is 71.5% and the standard deviation is 12.7%. It points to a generally wet environment in the centre of the polygons during sedimentation. Figure 6B shows the ice content anomaly curve in the polygon B. Significant changes of water content occurred when anomalies were equal to or greater (smaller) than one standard deviation above (below) the average.

The period from 2950 to 2750 cal. BP had the strongest WNW wind activity of the late Holocene, as indicated by a high loess content (Figure 6A), reflecting a stronger summer zonal atmospheric circulation. A marked and rapid decrease of WNW wind activity occurred after 2750 cal. BP, when the loess content quickly dropped under the average over only a few decades. This implies an abrupt shift of the summer wind regime that was followed by a marked decrease of ground moisture, characterized by strongly negative anomalies over a period of approximately 165 years where $\Delta ice < -1$ to $-2\,\sigma$.

Strongly negative loess contents anomalies, sometimes more than 2 standard deviations below the late Holocene average, indicate the establishment of a different summer surface wind

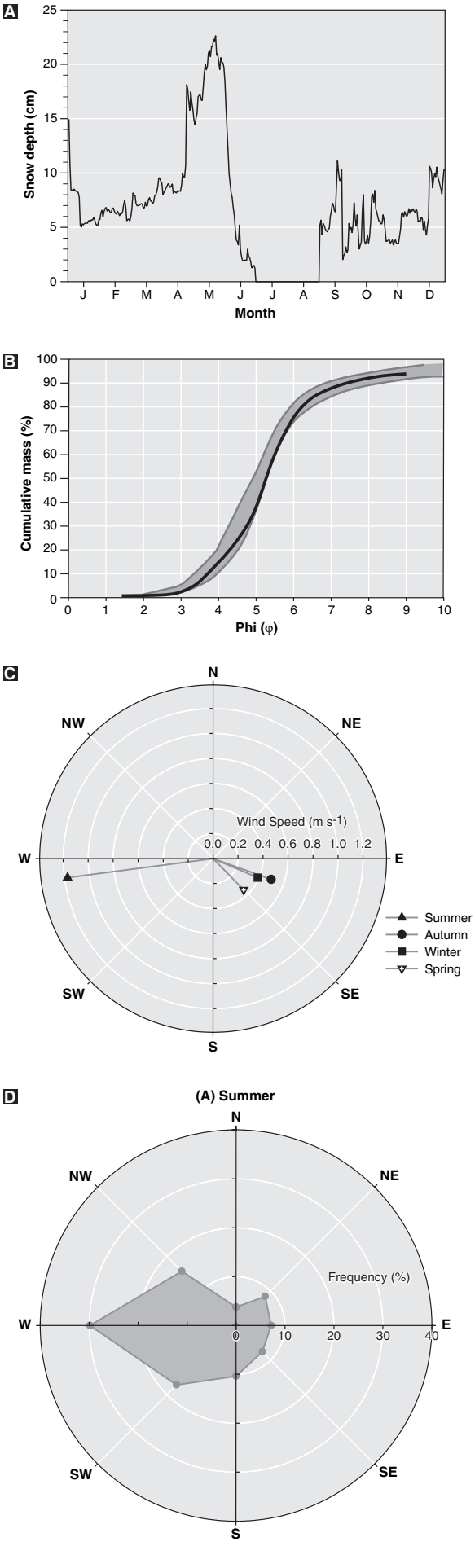

regime between 2450 and 2350 cal. BP. This was accompanied and followed by a strong increase of effective precipitation.

Two marked decreases of WNW winds occurred between 2050 cal. BP and 1850 cal. BP) as indicated by the strongly negative anomalies of loess contents (approximately 250 years where Δloess < -1 to $-2\ \sigma$). A significantly wetter episode occurred around 2050 cal. BP. It was followed by a brief phase that was drier than normal around 1850 cal. BP (Table 2). Strongly negative loess contents anomalies indicate a marked and sustained shift of summer surface wind regime after 1750 cal. BP. This was accompanied by a marked increase of P–E. Stronger WNW winds were accompanied by a gradual increase of P–E, particularly between 1350 and 1150 cal. BP (Δice $> 1\ \sigma$). As of 450 cal. BP, the rise in surface moisture conditions continued, a tendency that had begun around 850 cal. BP. The conditions were significantly wetter than average between 450 and 250 cal. BP (approximately 200 years where Δice $> 1\ \sigma$) and remained above the average afterwards up to 50 cal. BP.

Discussion

Syngenetic ice-wedge polygon development

The studied polygons represent sedimentary microbasins in which a sequence made up of pore ice, ice lenses, loess and organic matter has been accumulating since approximately 4000 cal. BP (polygon A). The development of these polygons stems from the regional climatic variations (temperature, precipitation, wind, evaporation) and from polygon-specific changes (ice-wedge growth causing microtopographical changes, drainage, exposure) (Lafarge-England *et al.*, 1991; Garneau, 2000). Cryoturbations associated with the growth of ice wedges and visco-plastic deformation of the sediments resulting from thermal expansion did not adversely deform the stratigraphy in the centre of the polygons.

The relatively synchronous variations of the accumulation rates ($R = 0.96$) of polygons A and B indicate a similar sedimentation during the late Holocene. In his study of sections along the river bluff, Allard (1996) also noticed the presence of rapid accumulation rates between *c*. 2564 and 2299 cal. BP and of slow rates thereafter for polygons located on the same terrace a few hundred metres from the study site. We deduce that synchronous stratigraphic changes within the polygons likely were the result of regional climatic changes (Gajewski *et al.*, 1995; Garneau, 2000).

The sandur was colonized between 3983 and 3472 cal. BP, as indicated by the dating of *Salix* spp. twigs recovered from the glaciofluvial sands at the stratigraphic contact with the peaty loess unit (Table 1: UL-2152, 2356). This colonization was the result of a change in the course of the proglacial river. This was probably due to the degradation of the river into its alluvial deposits following the isostatic uplift of this area of Bylot Island and to slower melting of upstream glaciers associated with cooler regional temperatures during the late Holocene (Fortier and Allard, 2004). This cooling was felt down to southeastern Canada and northeastern

Figure 5 (A) Average snow depth in the valley for the period 2001 to 2003. (B) Grain-size distribution of the loess retrieved from the polygons (shaded area) and of the silt from the sandur (solid line). Phi scale diameter. (C) Average seasonal wind direction at 3 m above the ground for the 1994–2003 period where the vector length represents the average directional wind speed. (D) Summer (June, July, August) wind direction frequency distribution over the study site (1994–2003). Figure 5A, C and D are courtesy of Gilles Gauthier, Laval University

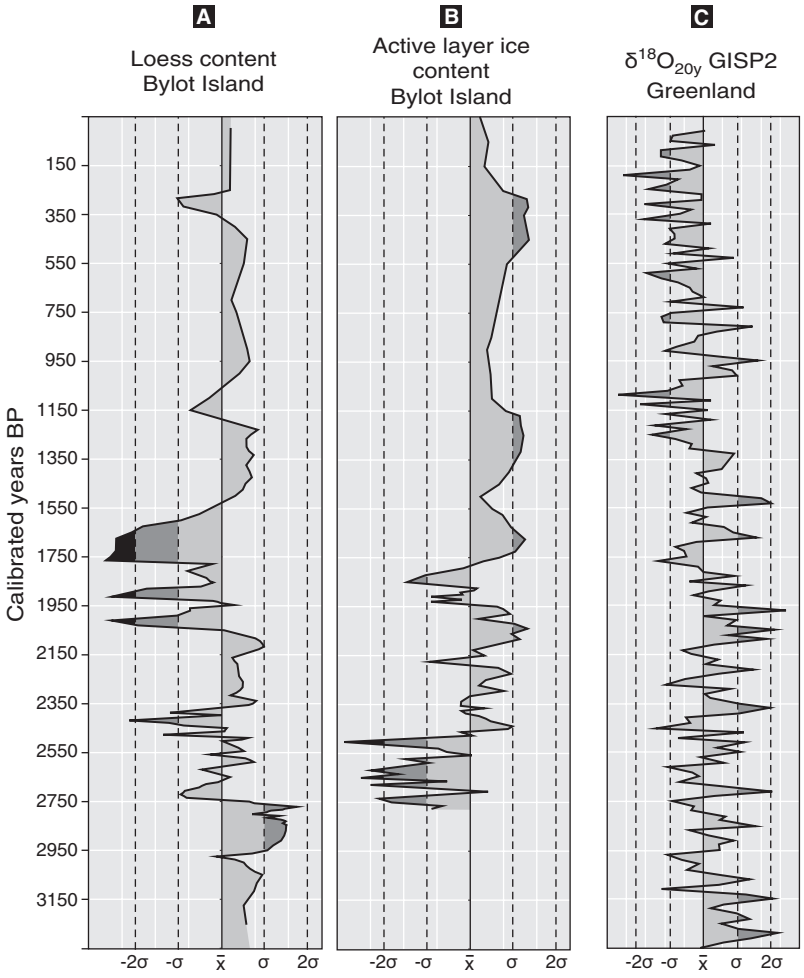

Figure 6 Anomalies of loess sedimentation and active-layer ice content during the late Holocene. The curves show the deviation from the average (standard deviation units). The dotted lines represent ± 1 or 2 standard deviations (σ) from the average. Dark grey shaded peaks show departure of ± 1 σ and black peaks ± 2 σ from the average, respectively. (A) Loess content in polygon B. Average = 72.4%, $\sigma = 12.7$. (B) Active-layer ice content in polygon B. Average = 71.5%, $\sigma = 12.7$. (C) GISP2 bidecennial oxygen isotope signal ($\delta^{18}O_{20y}$) from 3250 BP to 0 BP (GSIC, 1997). Average = $-34.84‰$, $\sigma = 0.34$

USA (Jackson *et al*., 1997). In the eastern Canadian Arctic archipelago and Greenland, it started around 3750–3350 cal. BP as suggested by glaciological data (Paterson *et al*., 1977; Koerner and Fisher, 1981; Bourgeois 1986; Stuiver *et al*., 1995; Domack and Mayewski, 1999; Stuiver and Grootes, 2000; Bourgeois *et al*., 2000) and various other palaeoclimatic indicators (Bradley, 1990; CAPE Project Members, 2001) such as peat accumulation rates (Garneau, 2000), diatoms (Wolfe, 2000; Joynt and Wolfe, 2001; Smith, 2002), marine mollusks assemblages (Dyke *et al*., 1996) and pollens (Fredskild, 1985; Short *et al*., 1985; Gajewski *et al*., 1995).

Late Holocene changes of summer surface wind regime and P–E balance of southwestern Bylot Island

We tentatively explain the changes of summer surface winds and P–E regimes recorded in the time series of loess and ice content in polygon B as the result of changes of the Canadian Polar Trough position during the late Holocene. These positions probably led to changes of cyclonic activity north and east of Baffin Island (Shabbar *et al*., 1997) and to recurrent synoptic types over some periods with specific surface wind, precipitation and air temperature regimes.

From 2950 to 2750 cal. BP, the climate was windier and probably warmer during the summer as indicated by less negative $\Delta\delta^{18}O_{20y}$ and the presence of ice layers resulting from snow summer melt at the top of the Greenland Ice Sheet around 2850 cal. BP (Alley and Anandakrishnan, 1995; GSIC, 1997) (Table 2).

From 2750 to 2350 cal. BP the air temperature did not follow any particular trend and was probably oscillating between colder and warmer spells (Figure 6C, Table 2). We presume that the drier (wetter) conditions likely resulted from reduced (increased) precipitation instead of increased (reduced) evaporation.

From 2100 to 1550 cal. BP, repeated shifts in the summer local atmospheric circulation are followed by shifts of P–E regimes from a wetter and probably warmer climate around 2100 cal. BP to drier and probably milder conditions around 1850 cal. BP, followed by a relatively rapid return to wetter conditions around 1750–1550 cal. BP (Herron *et al*., 1981; Alley and Anandakrishnan, 1995; Dahl-Jensen *et al*., 1998) (Table 2). This shows changing and oscillating summer surface wind and P–E regimes over short periods. McGowan *et al*. (2003) also reported an increase of the P–E signal of western Greenland lakes between 1950 and 1550 cal. BP.

A major shift of atmospheric circulation toward stronger summer surface WNW winds occurred after 1550 cal. BP and this was followed by wetter conditions until 1150 cal. BP. During this period, the air temperature was probably oscillating between colder and warmer spells (Paterson *et al*., 1977;

Table 2 Late Holocene reconstitution of major changes of summer surface wind regime, based on loess sedimentation, and active-layer moisture regime based on ice content, for the southwestern part of Bylot Island (see Figure 6A, B). Regional air temperatures were derived from the Greenland GISP2 bidecennial oxygen isotope data (see Figure 6C)

Cal. years BP	Wind regime (this study)	Active-layer moisture regime (this study)	Oxygen isotopes GISP2 ($\delta^{18}O_{20y}$)	Regional correlations[a]
550–250	Shift to weaker WNW winds	Wetter	Colder summers	8, 11, 12, 13, 14, 15, 16, 17, 18
1350–1150	Shift to stronger WNW winds (1550)	Wetter	Colder with warm spells	2, 3, 4, 5, 7, 8, 9,10
1750–1550	Shift to weakest WNW winds	Wetter	Colder–warmer	6
Around 1850	Shift to weak WNW winds	Drier	Milder summers	2, 5
Around 2050	Shift to weak WNW winds	Wetter	Warmer	1
2450–2350	Shift to weak WNW winds	Wetter	Colder–warmer	
2750–2450	Shift to weak WNW winds	Drier	Oscillating	3, 4
2950–2750	Strongest WNW winds	No data, sample loss	Warmer summers	1, 2

[a]Regional palaeoclimatological correlations are as follows: 1, more melt layers on Greenland Ice Sheet (GIS) (Alley and Anandakrishnan, 1995); 2, warmer on GIS (Dahl-Jensen *et al.*, 1998); 3, cold cycle around 2750 to 2650 and 1350 BP (Bond *et al.*, 1997); 4, cold lake temperatures, Bylot Island (Joynt and Wolfe, 2001); 5, more melt layers on GIS (DYE-3 borehole) (Herron *et al.*, 1981); 6, higher P–E signal, western Greenland lakes (McGowan *et al.*, 2003); 7, cold with warm spells on Greenland (O'Brien *et al.*, 1995); 8, cold eastern Canadian Arctic summers (Williams and Wigley, 1983); 9, warm spells on Devon Island Ice Cap (DIC) (Paterson *et al.*, 1977); 10, higher accumulation on GIS (Meese *et al.*, 1994); 11, extensive permanent snow cover on Baffin Island uplands (Falconer, 1966; Andrews *et al.*, 1976); 12, cold summers on Baffin Island (Andrews *et al.*, 1981); 13, extensive sea ice in Baffin Bay (450 to 250 BP) (Serreze *et al.*, 2000); 14, teleconnections with the NAO (Barlow, 2001; Glueck and Stockton, 2001); 15, lower DIC $\delta^{18}O$ values, fewer melt layers (400 to 250 BP) and summer accumulation on DIC (Koerner and Fisher, 1981, 1990); 16, fewer melt layers on GIS (Alley and Anandakrishnan, 1995); 17, fewer melt layers on GIS (DYE-3 borehole) (Herron *et al.*, 1981); 18, borehole temperature measurements show colder climate on GIS (Dahl-Jensen *et al.*, 1998).

Herron *et al.*, 1981; Williams and Wigley, 1983; O'Brien *et al.*, 1995; Bond *et al.*, 1997; Dahl-Jensen *et al.*, 1998; Joynt and Wolfe, 2001) (Figure 6, Table 2).

From 550 to 250 cal. BP, the P–E signal was definitely higher for a wetter climate. Several types of palaeoclimatic indicators showed that the beginning of the 'Little Ice Age' (LIA), a period characterized by a succession of cold decades interrupted by brief warm spells, would have started around 600 cal. BP (Williams and Wigley, 1983; Stuiver *et al.*, 1995, 1997; Christiansen, 1998; Stuiver and Grootes, 2000; Barlow, 2001). In the interval 400 to 50 BP, the regional climatic conditions were as a whole definitely colder than average (approximately 180 years where $\Delta\delta^{18}O_{20y} < -1$ to -2 σ; GSIC, 1997) with colder summers (Koerner, 1977; Bradley, 1990; Koerner and Fisher, 1990; Bradley and Jones, 1993; Jones and Bradley, 1995; Dahl-Jensen *et al.*, 1998; Grumet *et al.*, 2001). On Bylot Island, in the studied valley, glaciotectonic thrust plates were formed by an advance of glacier C-79 around 100 cal. BP in response to these cold temperatures (Klassen, 1982, 1993) (Table 1: GSC-3227). We propose that the wetter conditions between 550 and 250 cal. BP partly resulted from a snow-melt delay and reduced evaporation during colder summers (Table 2). Indeed, during this period, the snow cover was permanent during several decades and summers were apparently colder in some areas of Baffin Island and Greenland (Falconer, 1966; Andrews *et al.*, 1976, 1981; Overpeck *et al.*, 1997; Christiansen, 1998).

Conclusion

Following a detailed stratigraphic analysis ensuring that the strata are not adversely deformed by cryoturbations (Fortier and Allard, 2004), syngenetic ice-wedge polygons are used to reconstruct regional climatic oscillations. The polygons act as sedimentary basins recording the climate conditions. The complexity of the summer surface wind conditions and P–E regime in response to regional climatic variations and associated changes of atmospheric circulation makes interpretations challenging. However, major changes in the record were detected for some periods.

Significant changes in the summer surface wind and P–E regimes are observable during the last 3500 years. There was a high level of variability and a strong amplitude of the P–E regime and summer surface wind conditions on a decennial and secular timescale in general, but the climate that prevailed on Bylot Island at the end of the Holocene (3450 cal. BP to present) was characterized by a limited variability and amplitude of the regional MAAT, by a few degrees celsius or less. Major shifts of P–E regime were always associated with changes of summer surface wind regime, likely related to changes in atmospheric circulation. From 2950 to 2750 cal. BP, the summer climate was warmer and had the strongest northwesterly surface winds of the late Holocene. Shifts to a weaker northwesterly summer surface wind activity preceded the drier episodes that occurred from 2750 to 2450 and around 1850 cal. BP. The wetter episodes occurred from 2450 to 2350 cal. BP, around 2050, from 1750 to 1550, 1350 to 1150 and 550 to 250 cal. BP. However, there seems to be no linear relationship between P–E or summer surface wind regimes and air temperatures. Wet/Cold – Wet/Warm and Dry/Warm – Dry/Cold periods could probably be explained by the recurrence of particular synoptic types in response to changes in the CPT position during the late Holocene.

Given the abundance of sandurs bordered by syngenetic ice-wedge polygon networks in the Canadian Arctic archipelago, similar studies would help to reconstruct the surface wind regime on a regional basis for times before the instrumental period.

Acknowledgements

Special thanks must go to Dr Gilles Gauthier (Centre d'études nordiques) for access to his field camp during 1999, 2001 and 2002 and for making available instrumental climatological data. We are grateful to Isabelle Duclos, Christopher Ellis,

Stéphane Martel, Olivier Piraux and Denis Sarrazin for their field work support. Thanks to Dr Marie-Andrée Fallu and Cédric Paître for their valuable comments on a previous version of the text. The staff from Sirmilik National Park organized two public meetings where research activities were presented to the community of Pond Inlet and members of the Hunters and Trappers Organisation. Logistical support was provided by the Polar Continental Shelf Project (this paper is PCSP contribution 018-05) and Centre d'études nordiques. Financial support was provided by Natural Sciences and Engineering Research Council of Canada (NSERC-8410) to Michel Allard, by Fonds québécois de recherche sur la nature et les technologies (FQRNT) to Daniel Fortier and by the Northern Scientific Training Program of the Department of Indian and Northern Affairs to Daniel Fortier. The figures were drafted by Karine Tessier.

References

Allard, M. 1996: Geomorphological changes and permafrost dynamics: key factors in changing Arctic ecosystems. An example from Bylot Island, Nunavut, Canada. *Geoscience Canada* 23, 205–12.

Alley, R.B. and **Anandakrishnan, S.** 1995: Variations in melt-layer frequency in the GISP2 ice core: implication for Holocene summer temperatures in central Greenland. *Annals of Glaciology* 21, 64–70.

Alt, B.T. and **Maxwell, B.** 1990: The Queen Elizabeth Islands: a case study for Arctic climate data availability and regional climate analysis. In Harrington, C.R., editor, *Canada missing dimension*. Canadian Museum of Nature, 294–326.

—— 2000: Overview of the modern Arctic climate. In Garneau, M. and Alt, B.T., editors, *Environmental response to climate change in the Canadian High Arctic*. Geological Survey of Canada, Bulletin 529, 17–36.

Andrews, J.T., Davis, P.T. and **Wright, C.** 1976: Little Ice Age permanent snowcover in the Eastern Canadian Arctic: extent mapped from Landsat-1 Satellite Imagery. *Geografiska Annaler* 58A, 71–81.

Andrews, J.T., Davis, P.T., Mode, W.N., Nichols, H. and **Short, S.K.** 1981: Relative departure in July temperatures in northern Canada for the past 6000 yr. *Nature* 289, 164–67.

Bamzai, A.S. 2003: Relationship between snow cover variability and Arctic Oscillation Index on a hierarchy of time scales. *International Journal of Climatology* 23, 131–42.

Barlow, L.K. 2001: The time period A.D. 1400–1980 in central Greenland ice cores in relation to the North Atlantic sector. *Climatic Change* 48, 101–19.

Bond, G., Showers, W., Cheseby, M., Lotti, R., Almasi, P., deMenocal, P., Priore, P., Cullen, H., Hajdas, I. and **Bonani, G.** 1997: A pervasive millenial-scale cycle in North Atlantic Holocene and glacial climates. *Science* 278, 1257–66.

Bonsal, B.R., Shabbar, A. and **Higuchi, K.** 2001: Impacts of low frequency variability modes on Canadian winter temperature. *International Journal of Climatology* 21, 95–108.

Bourgeois, J.C. 1986: A pollen record from the Agassiz Ice Cap, northern Ellesmere Island, Canada. *Boreas* 15, 345–54.

Bourgeois, J.C., Koerner, R.M., Gajewski, K. and **Fisher, D.A.** 2000: A Holocene ice-core pollen record from Ellesmere Island, Nunavut, Canada. *Quaternary Research* 54, 275–83.

Bradley, R.S. 1990: Holocene paleoclimatology of the Queen Elizabeth Islands, Canadian High Arctic. *Quaternary Science Reviews* 9, 365–84.

Bradley, R.S. and **Jones, P.D.** 1993: 'Little Ice Age' summer temperature variations: their nature and relevance to recent global warming trends. *The Holocene* 3, 367–76.

Cadieux, M.-C., Gauthier, G., Berteaux, D., Gagnon, C. and **Lévesque, E.** 2005: Monitoring the environmental and ecological impacts of climate change on Bylot Island, Sirmilik National Park: 2004–2005 annual progress report. Unpublished report. Centre d'études nordiques, Université Laval.

CAPE Project Members 2001: Holocene paleoclimate data from the Arctic: testing models of global climate change. *Quaternary Science Reviews* 20, 1275–87.

Christiansen, H.H. 1998: 'Little Ice Age' nivation activity in northeast Greenland. *The Holocene* 8, 719–28.

Dahl-Jensen, D., Mosegaard, K., Gunderstrup, N., Clow, G.D., Johnsen, S.J., Hansen, A.W. and **Balling, N.** 1998: Past temperatures directly from the Greenland Ice Sheet. *Science* 282, 268–71.

Domack, E.W. and **Mayewski, P.A.** 1999: Bi-polar ocean linkages: evidence from late-Holocene Antarctic marine and Greenland ice-core records. *The Holocene* 9, 247–51.

Duclos, I. 2002: Milieux mésiques et secs de l'Île Bylot, Nunavut (Canada): caractérisation et utilisation par la Grande oie des neiges. M.Sc. Thesis, Université du Québec à Trois-Rivières.

Dyke, A.S., Hooper, J. and **Savelle, J.M.** 1996: A history of sea ice in the Canadian Arctic Archipelago based on postglacial remains of the Bowhead whale (*Balaena mysticetus*). *Arctic* 49, 235–55.

Ellis, C.J. and **Rochefort, L.** 2004: Century-scale development of polygon-patterned tundra wetland, Bylot Island (73°N, 80°W). *Ecology* 85, 963–78.

Environment Canada 2002: *Canadian climate normals, 1971–2000. The North-Nunavut, Pond Inlet.* Environment Canada, Atmospheric Environment Service. Retrieved 10 April 2006 from http://www.climate.weatheroffice.ec.gc.ca/climate_normals

Falconer, G. 1966: Preservation of vegetation and patterned ground under a thin ice body in northern Baffin Island, N.W.T. *Geographical Bulletin* 8, 194–200.

Fortier, D. 2005: Évolution géomorphologique holocène des polygons à coins de glace de la vallée du glacier C-79, Ile Bylot, archipel arctique canadien. Ph.D. Thesis, Université Laval.

Fortier, D. and **Allard, M.** 2004: Late Holocene syngenetic ice-wedge polygons development, Bylot Island, Canadian Arctic Archipelago. *Canadian Journal of Earth Sciences* 41, 997–1012.

—— 2005: Frost-cracking conditions, Bylot Island, Canadian Arctic Archipelago. *Permafrost and Periglacial Processes* 16, 145–61.

Fredskild, B. 1985: Holocene pollen records from west Greenland. In Andrews, J.T., editor, *Quaternary environments, eastern Canadian Arctic, Baffin Bay and western Greenland*. Allen and Unwin, 643–81.

Frei, A. and **Robinson, D.A.** 1999: Northern hemisphere snow extent: regional variability 1972–1994. *International Journal of Climatology* 19, 1535–60.

Gagnon, C.A., Cadieux, M.-C., Gauthier, G., Lévesque, E., Reed, A. and **Berteaux, D.** 2004: Analyses and reporting on 15 years of biological monitoring from Bylot Island, Sirmilik National Park of Canada. Unpublished report. Centre d'études nordiques, Université Laval.

Gajewski, K., Garneau, M. and **Bourgeois, J.C.** 1995: Paleoenvironments of the Canadian High Arctic derived from pollen and plant macrofossils: problem and potentials. *Quaternary Science Reviews* 14, 609–29.

Garneau, M. 1992: Analyses macrofossiles d'un dépot de tourbe dans la région de Hot Weather Creek, péninsule de Fosheim, Île d'Ellesmere, Territoire du Nord-Ouest. *Géographie physique et Quaternaire* 46, 285–94.

—— 2000: Peat accumulation and climatic change in the High Arctic. In Garneau, M. and Alt, B.T., editors, *Environmental response to climate change in the Canadian High Arctic*. Geological Survey of Canada, Bulletin 529, 283–93.

Glueck, M.F. and **Stockton, C.W.** 2001: Reconstruction of the North Atlantic Oscillation, 1429–1983. *International Journal of Climatology* 21, 1453–65.

Greenland Summit Ice Cores CD-ROM 1997: National Snow and Ice Data Center, University of Colorado at Boulder.

Grootes, P.M., Stuiver, M., White, J.W.C., Johnsen, S. and **Jouzel, J.** 1993: Comparison of oxygen isotope records from the GISP2 and GRIP ice cores. *Nature* 366, 552–54.

Grumet, N.S., Wake, C.P., Mayewski, P.A., Zielinski, G.A., Whitlow, S.I., Koerner, R.M., Fisher, D.A. and **Woolleett, J.M.** 2001: Variability of sea-ice extent in Baffin Bay over the last millenium. *Climatic Change* 49, 129–45.

Herron, M.M., Herron, S.L. and **Langway, C., Jr** 1981: Climatic signal of ice melt features in southern Greenland. *Nature* 293, 389–91.

Hurrell, J.W. 1995: Decadal trends in the North Atlantic Oscillation: regional temperatures and precipitation. *Science* 269, 676–79.

Inland Waters Branch 1969: *Glacier atlas of Canada, Bylot Island Area, 46201*. Environment Canada.

Jackson, S.T., Overpeck, J.T., Webb, T., III, Keattch, S.E. and **Anderson, K.H.** 1997: Mapped plant-macrofossil and pollen records of Late Quaternary vegetation change in Eastern North America. *Quaternary Science Reviews* 16, 1–70.

Jones, P.D. and **Bradley R.S.** 1995: Climatic variations over the last 500 years. In Bradley, R.S. and Jones, P.D., editors, *Climate since AD 1500*. Routledge, 649–65.

Joynt, E.H., III and **Wolfe, A.P.** 2001: Paleoenvironmental inference models from sediment diatom assemblages in Baffin Island lakes (Nunavut, Canada) and reconstruction of summer water temperature. *Canadian Journal of Fisheries and Aquatic Sciences* 58, 1222–43.

Kapsner, W.R., Alley, R.B., Shuman, C.A., Anandakrishnan, S. and **Grootes, P.M.** 1995: Dominant influence of atmospheric circulation on snow accumulation in Greenland over the past 18,000 years. *Nature* 373, 52–54.

Kasper, J. and **Allard, M.** 2001: Late Holocene climatic changes as detected by the growth and decay of ice wedges on the southern shore of Hudson Strait, northern Québec, Canada. *The Holocene* 11, 563–77.

Klassen, R.A. 1982: *Glaciotectonic thrust plates, Bylot Island, District of Franklin*. Geological Survey of Canada, Current Research, Paper 82-1A, 369–73.

—— 1993: *Quaternary geology and glacial history of Bylot Island, Northwest Territories*. Geological Survey of Canada, Memoir 429.

Koerner, R.M. 1977: Devon Island Ice Cap: core stratigraphy and paleoclimate. *Science* 196, 15–18.

Koerner, R.M. and **Fisher, D.A.** 1981: Studying climatic change from Canadian high Arctic cores. In Harrington, C.R., editor, *Climatic change in Canada 2*. Syllogeus 31, 195–218.

—— 1990: A record of Holocene summer climate from a Canadian high-Arctic ice core. *Nature* 343, 630–31.

Lafarge-England, C., Vitt, D.H. and **England, J.** 1991: Holocene soligenous fens on a High Arctic fault block, Northern Ellesmere Island 82N, N.W.T., Canada. *Arctic and Alpine Research* 23, 80–98.

Lockwood, J.G. 2001: Abrupt and sudden climatic transitions and fluctuations: a review. *International Journal of Climatology* 21, 1153–79.

Mackay, J.R. 1975: *The stability of permafrost and recent climatic change in the Mackenzie valley, N.W.T.* Geological Survey of Canada, Current Research, Paper 75-1B, 173–76.

—— 1980: *Deformations of ice-wedge polygons, Garry Island, Northwest Territories*. Geological Survey of Canada, Current Research, Paper 80-1A, 287–91.

—— 1990: Some observation on the growth and deformation of epigenetic, syngenetic and anti-syngenetic ice-wedges. *Permafrost and Periglacial Processes* 1, 15–29.

—— 2000: Thermally induced movements in ice-wedge polygons, western Arctic coast: a long-term study. *Géographie physique et Quaternaire* 54, 41–68.

Marshall, J., Kushnir, Y., Battisti, D., Chang, P., Czaja, A., Dickson, R., Hurrell, J., McCartney, M., Saravanan, R. and **Visbeck, M.** 2001: North Atlantic climate variability: phenomena, impacts and mechanisms. *International Journal of Climatology* 21, 1863–98.

Massé, H. 1998: Estimation de la capacité de support des différents écosystèmes humides utilisés par la grande oie des neiges nichant à l'île Bylot (Nunavut, Canada). M.Sc. Thesis. Université Laval.

Maxwell, J.B. 1980: *The climate of the Canadian Arctic islands and adjacent waters*. Atmospheric Environment Service, Environment Canada.

—— 1981: Climatic regions of the Canadian Arctic islands. *Arctic* 34, 225–40.

McGowan, S., Ryves, D.B. and **Anderson, N.J.** 2003: Holocene records of effective precipitation in west Greenland. *The Holocene* 13, 239–49.

Meese, D.A., Gow, A.J., Grootes, P., Mayewski, P.A., Ram, M., Stuiver, M., Taylor, K.C., Waddington, E.D. and **Zielinski, G.A.** 1994: The accumulation record from the GISP2 core as an indicator of climate change throughout the Holocene. *Science* 266, 1680–82.

Mote, T.L. 1998a: Mid-tropospheric circulation and surface melt on the Greenland Ice Sheet. Part I: atmospheric teleconnections. *International Journal of Climatology* 18, 111–29.

—— 1998b: Mid-tropospheric circulation and surface melt on the Greenland Ice Sheet. Part II: synoptic climatology. *International Journal of Climatology* 18, 131–45.

New, M., Todd, M., Hulme, M. and **Jones, P.** 2001: Precipitation measurements and trends in the twentieth century. *International Journal of Climatology* 21, 1899–922.

O'Brien, S.R., Mayewski, P.A., Meeker, L.D., Meese, D.A., Twickler, M.S. and **Whitlow, S.I.** 1995: Complexity of Holocene climate as reconstructed from a Greenland ice core. *Science* 270, 1962–64.

Overpeck, J.T., Hughen, K., Bradley, R., Case, R., Douglas, M., Finney, B., Gajewski, K., Jacoby, G., Jennings, A., Lamoureux, S., Lasca, A., MacDonald, G., Moore, J., Retelle, M., Smith, S., Wolfe, A. and **Zielinski, G.** 1997: Arctic environmental change of the last four centuries. *Science* 278, 1251–56.

Paterson, W.S.B., Koerner, R.M., Fisher, D., Johnsen, S.J., Clausen, H.B., Dansgaard, W., Bucher, P. and **Oeschger, H.** 1977: An oxygen-isotope climatic record from the Devon Island Ice Cap, Arctic Canada. *Nature* 266, 508–11.

Pryzbylak, R. 2000: Temporal and spatial variation of surface air temperature over the period of instrumental observations in the Arctic. *International Journal of Climatology* 20, 587–614.

Romanovsky, V.E. and **Osterkamp, T.E.** 1997: Thawing of the active layer on the coastal plain of the Alaskan Arctic. *Permafrost and Periglacial Processes* 8, 1–22.

Seppälä, M., Gray, J. and **Ricard, J.** 1991: Development of low-centred ice-wedge polygons in the northernmost Ungava Peninsula, Québec, Canada. *Boreas* 20, 259–82.

Serreze, M.C., Walsh, J.E., Chapin, F.S., III, Osterkamp, T.E., Dyurgerov, M., Romanovsky, V., Oechel, W.C., Morison, J., Zhang, T. and **Barry R.G.** 2000: Observational evidence of recent change in the northern high-latitude environment. *Climatic Change* 46, 159–207.

Shabbar, A., Higuchi, K., Skinner, W. and **Knox, J.L.** 1997: The association between the BWA index and winter surface temperature variability over eastern Canada and west Greenland. *International Journal of Climatology* 17, 1195–210.

Short, S.K., Mode, W.N. and **Davis, P.T.** 1985: The Holocene record from Baffin Island: modern and fossil pollen studies. In Andrews, J.T., editor, *Quaternary Environments, eastern Canadian Arctic, Baffin Bay and western Greenland*. Allen and Unwin, 608–42.

Smith, I.R. 2002: Diatom-based Holocene paleoenvironmental records from continental sites on the north-eastern Ellesmere Island, high Arctic, Canada. *Journal of Paleolimnology* 27, 9–28.

Stuiver, M. and **Grootes, P.M.** 2000: GISP2 oxygen isotope ratios. *Quaternary Research* 53, 277–84.

Stuiver, M. and **Reimer, P.J.** 1993: University of Washington Quaternary isotope lab radiocarbon calibration program rev 4.3. *Radiocarbon* 35, 215–30.

Stuiver, M., Grootes, P.M. and **Braziunas, T.F.** 1995: The GISP2 $\delta^{18}O$ climate record of the past 16 500 years and the role of the sun, ocean and volcanoes. *Quaternary Research* 44, 341–54.

Stuiver, M., Braziunas, T.F., Grootes, P.M. and **Zielinski, G.A.** 1997: Is there evidence for solar forcing of climate in the GISP2 oxygen isotope record? *Quaternary Research* 48, 259–66.

Stuiver, M., Reimer, P.J., Bard, E., Beck, J.W., Bur, G.S., Hughen, K.A., Kromer, B., McCorman, G., Van Der Plicht, J. and **Spurk, M.** 1998: INTCAL98 radiocarbon age calibration, 24,000–0 cal BP. *Radiocarbon* 40, 1041–83.

Taylor, K.C., Lamorey, G.W., Doyle, G.A., Alley, R.B., Grootes, P.M., Mayewski, P.A., White, J.W.C. and **Barlow, L.K.** 1993: The 'flickering switch' of Late Pleistocene climate change. *Nature* 361, 432–36.

Vanderberghe, J. 1991: Changing conditions of aeolian sand deposition during the last deglaciation period. *Zeitschrift für Geomorphologie N.F. Supplement Band* 90, 193–207

Williams, L.D. and **Wigley, T.M.L.** 1983: A comparison of evidence for Late Holocene summer temperature variations in the northern hemisphere. *Quaternary Research* 20, 286–307.

Wolfe, A.P. 2000: A 6500-year diatom record from southwestern Fosheim Peninsula, Ellesmere Island, Nunavut. In Garneau, M. and Alt, B.T., editors, *Environmental response to climate change in the Canadian High Arctic*. Geological Survey of Canada, Bulletin 529, 249–56.

Zhang, T. and **Stamnes, K.** 1998: Impacts of climatic factors on the active layer and permafrost at Barrow, Alaska. *Permafrost and Periglacial Processes* 9, 229–46.